# PROTOYPE INSTRUMENT EMPLOYING AN INTEGRATED ARRAY OF POLYMER-COATED FLEXURAL-PLATE-WAVE (FPW) VAPOR SENSORS

Q. Y. Cai, D. Heldsinger, M. D. Hsieh, J. Park, and E. T Zellers*
Department of Environmental Health Sciences and Department of Chemistry
University of Michigan, Ann Arbor, MI 48109-2029
Email: ezellers@umich.edu

Preliminary testing of a prototype instrument employing an integrated array of six polymer-coated flexural plate wave (FPW) sensors and an adsorbent preconcentrator is described. Measurements of eight vapors individually and in selected binary and ternary mixtures were collected. Responses were linear with concentration and mixture responses were equivalent to the sums of the component vapor responses. Limits of detection as low as 0.3 ppm were achieved from a 60-sec (200 $cm^3$) air sample. Increases in sampling flow rates (volumes) led to commensurate increases in responses. However, for a given sample volume, increases in the desorption flow rate led to decreases in response maxima indicating that sorption kinetics limit responses at higher flow rates. Modeling of array performance using Monte Carlo simulations indicate that all individual vapors and certain 2° and 3° mixtures could be recognized/discriminated with very low error. More complex mixtures, and those containing homologous vapors, were problematic.

## INTRODUCTION

Arrays of partially selective sensors can be used to analyze multiple vapors. In most reports, the chemically sensitive interface materials employed are polymers of different structures into which vapors reversibly partition to varying degrees. The differential partitioning gives rise to the characteristic response pattern used for vapor recognition. This approach to array design has been reported for several vapor sensor technologies (1-5).

The flexural-plate-wave (FPW) sensors described here are similar in many respects to the more common surface-acoustic-wave SAW sensors (6-10). In both sensors, radio-frequency mechanical (acoustic) waves are generated within a piezoelectric substrate that has been coated with a chemically sensitive (e.g., polymer) film. The acoustic waves are launched and received by a pair of interdigital transducers (IDTs) on the device surface, and a feedback amplifier connecting the IDTs permits sustained oscillation at a frequency determined by the device structure. Small changes in the mass or viscoelastic properties of the coating film caused by interactions with gases or vapors result in a change of the acoustic wave velocity, which can be measured indirectly as a change in wave frequency using digital frequency counting electronics.

In the FPW device the active region on which the acoustic waves travel is a membrane whose thickness is much smaller than the acoustic wavelength (6-10). For chemical sensing the polymer-coated FPW device has the advantages of supporting thick polymer layers without loss of oscillation, low operating frequency, silicon-based fabrication, and environmental isolation of the electrodes. Although individual polymer-coated FPW vapor sensors have been reported (6-9), there has yet to be a report of vapor sensing with an integrated array of FPW sensors.

Where measurement of trace concentrations of organic vapors in the ambient environment are required, preconcentration, via a bed of a hydrophobic granular porous polymer, is helpful to increase sensitivity, provide drift compensation, and provide a degree of water-vapor compensation (11-13).

In this article, preliminary testing of an instrument employing an integrated array of six FPW sensors and an adsorbent preconcentrator is described. One of the sensors failed during initial experiments, so results are reported here for only five sensors. Results of calibrations of several organic solvent vapors, individually and in simple mixtures, are described. These data are then used in Monte Carlo simulations coupled with pattern recognition analyses to assess the capabilities for vapor recognition and discrimination. The effects of varying the sampling and desorption flow rates on sensor responses are discussed as well as other operating features of the instrument.

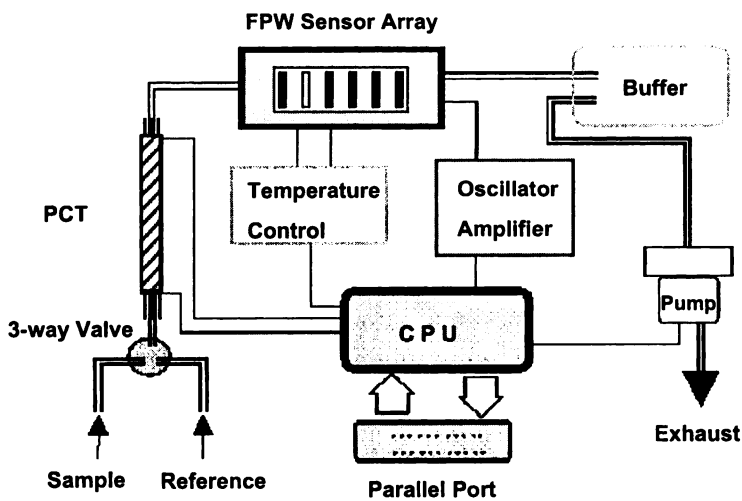


Figure 1. Block diagram of key prototype instrument components.

## METHODS

The prototype instrument (23×23×5 cm) operates on AC power and contains the FPW array, a miniature adsorbent preconcentrator, sampling pump, and control and drive electronics (Figure 1). A laptop computer coordinates the system operation, and processes and displays the sensor outputs in near real time. A manual, low-dead-volume, 3-way valve was affixed to the inlet of the instrument for this study to allow switching between vapor test-atmospheres and clean, dry air. The instrument was designed and constructed by Berkeley MicroInstruments (Richmond, CA).

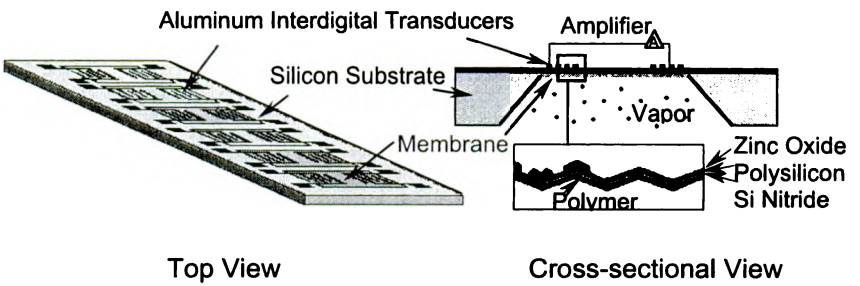


Figure 2. Integrated FPW 6-sensor array and structure of individual sensor.

Each FPW device membrane is a layered composite attached along its periphery to a silicon substrate, and the IDTs are patterned directly on the membrane, which flexes upon excitation (Figure 2). The devices were fabricated on membranes 5 μm thick consisting of a silicon nitride layer, a polished layer of p-doped polysilicon, and a ZnO piezoelectric layer. The IDT electrodes were patterned to give an acoustic wavelength of 80 mm and a resonant frequency of 8 MHz. Each device is operated as an oscillator by sequential connection to a single feedback amplifier. The six FPW devices are integrated on a single chip measuring 8 mm × 12 mm and bonded into a hybrid integrated-circuit package. Frequency measurements are mixed with a reference signal from a local oscillator (LO) generated by a direct digital synthesizer.

A large aperture cut in the underside of the IC package exposes the backside of the FPW array membranes for interfacial coating application and vapor exposure testing, and the entire assembly is inverted so that the exposed membranes are facing upwards. The front side of the sensor array chip and the bond wires to the package are isolated from the environment. Vapors are delivered via a manifold machined to fit into the aperture in the package, forming a detector cell with a ~20-mL dead volume (i.e., ~3μL per sensor). The array package is heated to 30 °C with a resistive heater on the manifold.

The preconcentrator is a 200-mL glass capillary packed with approximately ~20 mg of 60/80 mesh Tenax® GR granular adsorbent held in place with steel wool. A gold-wire resistive heater wrapped along the length of the capillary provides rapid heating and flash desorption of collected vapors.

The onboard diaphragm pump draws a sample through the preconcentrator and over the sensor array at a flow rate between 8 and 36 mL/min. The preconcentrator retains the incoming vapors as well as a fraction of the incoming water vapor from the matrix of air at 50% relative humidity used in all tests. After a predefined sampling period the preconcentrator is flash heated and the vapors are desorbed and distributed over the sensors in the array. The maxima of the eluting peaks are used for quantification and response pattern generation.

A set of polymer coatings was selected using linear-solvation-energy-relationship (LSER) concepts to span a broad range of functional groups (14,15). These included polyisobutylene (PIB), polyepichlorohydrin (PECH), polydiphenoxyphosphazene (PDPP), phenylmethyldiphenylsilicone (OV-25), bis-cyanyoallyl polysiloxane (OV-275), and fluoropolyol (FPOL). Each polymer was applied by airbrush as a solution in a volatile solvent (0.2 %w/v) while monitoring the sensor frequency. However, adherent coatings of OV-25 could not be obtained despite various attempts to promote adhesion. It was, therefore, replaced with a side-chain liquid crystalline polymer (SCLCP) whose structure and properties are described elsewhere (16). The thickness of the coating film on each sensor was estimated from the frequency shift and ranged from 0.57 μm (FPOL) to 1.08 μm (OV-275) (9). Shortly after coating, the PIB-coated sensor failed and could not be resurrected.

Table I lists the eight solvent vapors tested and the range of vapor concentrations over which the instrument was calibrated. Three binary mixtures and three ternary mixtures of subsets of these vapors were also tested.

The Monte Carlo simulations were generated using an error model described elsewhere (5,15), which accounts for variations in sample volume, desorption heating rate, baseline noise, residual water vapor in desorbed samples, and calibration procedures. All of these factors were quantified experimentally. The population of error-enhanced synthetic responses is sampled iteratively and each sample is treated as an unknown that is then assigned an identity by comparison with the response patterns established from the calibration data. Pattern recognition analysis entailed extended disjoint principal components regression (EDPCR) (5,12,15). The number and nature of recognition errors observed from a large sample set (i.e., hundreds of simulations) were logged and evaluated.

## RESULTS

### Response Characteristics

Response profiles were highly reproducible among replicate trials, with relative standard deviations of the maxima of four replicates at a given concentration typically ranging from 0.6 to 3.5% . Vapor responses were linear with concentration ($r^2 \geq 0.98$) in all cases. Responses to vapor mixtures were equivalent to the sum of the responses of the component vapors. Peak shapes varied among the sensors, reflecting the relative vapor sorption/desorption kinetics. Peak widths (full width at half-maximum) at 34 mL/min ranged from 0.8 to 3.6 sec, being wider for the less volatile vapors and for vapors giving larger responses. The PDPP-coated sensor gave the narrowest and most symmetric peaks, while those for the SCLCP- and FPOL-coated sensors were broader and showed

significant tailing indicative of slow diffusion of vapors in these coatings, which has been noted previously for these sensor coatings (16,17). Peaks for the sensors coated with PECH and OV-275 were intermediate in width and symmetry. Peaks corresponding to water vapor eluted prior to those for the organic vapors, with partial overlap observed for the earlier eluting vapors.

Table I shows the matrix of sensitivities and LODs for a 60-sec sample at a flow rate (sampling and desorption) of 34 mL/min. The sensitivities are quite high compared to SAW sensors coated with the same polymers operated under similar conditions (i.e., with preconcentration) (5,11,12), owing to the relatively thick polymer layers employed, the efficiency of thermal desorption of preconcentrated samples, and the low dead volume of the sensor array. However, the baseline noise levels for these sensors, which ranged from 30-85 Hz (rms), are also quite high and the resulting LODs are greater than expected. The major source of baseline noise was found to be the instrument pump. With the pump off, baseline noise levels were reduced to 1-2 Hz (rms). Better isolation of the pump should lead to significant improvements in LODs. Repeated calibrations with toluene over a 6-week period indicated no changes in response characteristics.

Table I. Sensitivities and LODs for the test vapors.[a]

| Vapor | Conc. range[b] | Sensitivity[c] (LOD[d]) SCLCP | FPOL | PDPP | PECH | OV-275 |
|---|---|---|---|---|---|---|
| benzene [BEN] | 50-600 | 8.8 (13) | 43.9 (6.1) | 123 (1.6) | 163 (1.1) | 28.9 (5.9) |
| toluene [TOL] | 40-210 | 21.5 (5.5) | 76.8 (3.5) | 151 (1.3) | 252 (0.7) | 43.1 (3.9) |
| m-xylene [XYL] | 36-200 | 45.3 (2.6) | 144 (1.9) | 246 (0.8) | 421 (0.4) | 74.5 (2.3) |
| trichloroethylene [TCE] | 50-250 | 8.5 (14) | 24.8 (11) | 55.6 (3.6) | 64.1 (2.8) | 14.1 (12) |
| perchloroethylene [PCE] | 40-250 | 23.2 (5.1) | 77.0 (3.5) | 218 (0.9) | 182 (1.0) | 52.5 (3.2) |
| 2-butanone [MEK] | 50-400 | 10.8 (11) | 467 (0.6) | 102 (1.9) | 260 (0.7) | 43.9 (3.9) |
| n-butylacetate [BAC] | 50-400 | 25.2 (4.7) | 880 (0.3) | 132 (1.5) | 477 (0.4) | 63.6 (2.7) |
| 2-propanol [IPA] | 50-450 | 1.6 (75) | 58.5 (4.6) | 9.0 (22) | 20.6 (8.6) | 10.5 (16) |
| water[e] | | 0.011 | 0.079 | 0.010 | 0.042 | 0.035 |

[a] 34mL/min, 60-sec sample; RH= 50%; [b] ppm; [c]Hz/ppm; [d] ppm, [e] 50% RH.

## Sample Volume and Flow Rate Effects

Increasing the sampling and desorption flow rates led to proportional increases in sensitivity as shown for xylene in Figure 3 for flow rates of 11 and 34 mL/min (60-sec sample). If the sampling time at a given flow rate is increased, the sensitivity also increases proportionally. However, for a flow rate of 34 mL/min, increasing the sampling time beyond 3 min resulted in apparent breakthrough of the preconcentrator: the sensitivity increased at a reduced rate at longer sampling times. Interestingly, for a fixed sampling volume, if the desorption flow rate is increased, the sensitivity decreases even though the elution time and peak width also decrease. At a fixed sample volume of 160 mL, for example, increasing the desorption flow rate from 8 to 36 mL/min leads to

reductions in responses to toluene of ~40-60% among the five sensors. This indicates that sorption kinetics limit responses at the higher flow rates.

As the flow rate is increased from 8 to 36 mL/min the sample residence time within each sensor decreases from 135 to 30 ms. Assuming diffusional mass transport within the coating films, for a film thickness range of 0.6 to 1.0 μm and an assumed diffusion coefficient of $10^{-7}$ $cm^2$/sec, the time for the vapor to diffuse through the coating film ranges from about 9-25 ms. Thus, diffusion times are of the same order as sample residence times above the sensors, and it is reasonable to conclude that sorption equilibrium is not being reached at the higher flow rates.

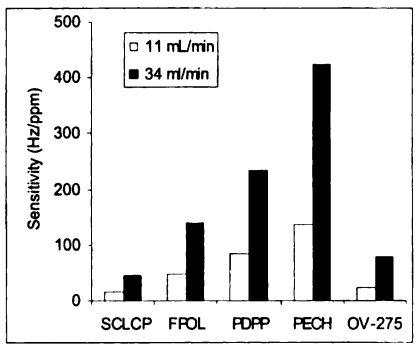


Figure 3. Effect of sampling flow rate (volume) on sensitivity to xylene.

Performance Modeling

Modeling of array performance was explored using Monte Carlo simulations coupled with EDPCR pattern recognition analysis. The first case considered was where the responses to an individual vapor are being analyzed and it must be recognized as one of the eight calibrated vapors (no mixtures were considered). The procedure of generating synthetic responses and assigning identities was performed 500 times for each of eight vapors (i.e., 4000 simulations) to obtain a stable statistical estimate of the reliability of recognition. The allowed concentration range was 3 – 30 × LOD, where the LOD was defined as that corresponding to the least sensitive sensor in the array for the specific vapor under consideration. Table II shows the results of this analysis by vapor in the form of a recognition matrix. The only significant errors in recognition occur between toluene and m-xylene. The predicted average recognition rate is 98.7%.

Table II. Recognition matrix (n=500 simulations) from EDPCR/Monte Carlo modeling of the 5-sensor array.

| | BEN[a] | TOL | XYL | TCE | PCE | MEK | BAC | IPA |
|---|---|---|---|---|---|---|---|---|
| BEN[b] | 500 | 2 | 0 | 0 | 1 | 0 | 0 | 0 |
| TOL | 0 | 480 | 31 | 1 | 0 | 0 | 0 | 0 |
| XYL | 0 | 18 | 469 | 0 | 0 | 0 | 0 | 0 |
| TCE | 0 | 0 | 0 | 499 | 0 | 0 | 0 | 0 |
| PCE | 0 | 0 | 0 | 0 | 499 | 0 | 0 | 0 |
| MEK | 0 | 0 | 0 | 0 | 0 | 500 | 1 | 0 |
| BAC | 0 | 0 | 0 | 0 | 0 | 0 | 499 | 0 |
| IPA | 0 | 0 | 0 | 0 | 0 | 0 | 0 | 500 |
| Recog. (%) | 100 | 96.0 | 93.8 | 99.8 | 99.8 | 100 | 99.8 | 100 |

a: actual identities in columns, b: assigned identities in rows.

To explore the performance of the instrument where mixtures of vapors could be present, several additional series of simulations were performed. Subsets of two, three, four, or five vapors were selected from the eight vapors on the basis of cluster analyses and Table II to span the range of difficulty in recognition expected for the data set. Mixture analyses considered the recognition and discrimination of all possible sub-components of a vapor subset of a given size. For subsets of two, three, four, and five vapors, the number of possible sub-components is 3, 7, 15, and 31, respectively. Six subsets of two vapors, six subsets of three vapors, three subsets of four vapors, and three subsets of five vapors were analyzed. Results are shown in Table III. Recognition rates range from 72-97% for the subsets of two vapors. For subsets of similar vapors, rates are lower than for subsets of vapors from different classes as expected. For the subsets of three vapors, recognition rates range from 60-93% and show the same trends with subset composition as for the 2-vapor subsets. Errors in recognition become significant where subsets of four or more vapors are considered indicating that reliable performance would not be possible for any of these cases.

Table III. Predicted recognition rates for specific vapor subsets.

| # of vapors | Vapor subset | Recog. rate (%) | # of vapors | Vapor subset | Recog. rate (%) |
|---|---|---|---|---|---|
| 2 | MEK+IPA | 94.9 | 3 | TOL+PCE+IPA | 92.9 |
| | XYL+BAC | 96.9 | | MEK+BAC+IPA | 76.1 |
| | TCE+BEN | 86.7 | | BEN+TOL+XYL | 52.7 |
| | TOL+TCE | 86.5 | | TOL+XYL+TCE | 59.5 |
| | TOL+XYL | 72.4 | | TCE+PCE+MEK | 75.0 |
| | MEK+BAC | 83.1 | | BAC+BEN+PCE | 86.0 |
| 4 | BEN+TOL+XYL+TCE | 42.2 | 5 | BEN+TOL+XYL+TCE+PCE | 28.9 |
| | TOL+TCE+XYL+PCE | 42.4 | | MEK+BAC+IPA+BEN+PCE | 52.4 |
| | TOL+PCE+MEK+IPA | 80.7 | | IPA+MEK+PCE+BEN+XYL | 61.0 |

## CONCLUSIONS

This is the first report on the use of an integrated array of polymer-coated FPW sensors for multi-vapor analysis. Results indicate that the instrument provides highly sensitive, stable responses and that unique response patterns are obtained for individual vapors. Increases in sampling flow rates lead to commensurate increases in responses. However, for a given sample volume, increases in desorption flow rates lead to decreases in responses indicating that sorption kinetics limit responses at high flow rates. Sub-ppm LODs are achievable for several vapors with a 60-sec sampling time. Improvements in LODs by an order of magnitude are expected by better vibration isolation of the sampling pump in the instrument.

## ACKNOWLEDGMENTS

The authors are indebted to S. Wenzel, B. Costello, and E. Snyder for technical assistance and valuable discussions, and to A. Snow for providing a sample of FPOL. Funding was provided by Grant R01-OH03692 from the National Institute for Occupational Safety and Health of the Centers for Disease Control and Prevention (NIOSH-CDCP) and by a subcontract from Berkeley MicroInstruments, Inc. (U. S. Air Force SBIR Grant F0865-93-C-0096).

## REFERENCES

1. E. T. Zellers, S. Batterman, M. Han, S. J. Patrash, *Anal. Chem.* **67**, 1092 (1995).
2. B. J. Doleman, M. Lonergan, E. Severin, T. Vaid, N. Lewis, *Anal. Chem.* **70**, 4177 (1998).
3. W. P. Carey, K. Beebe, B. R. Kowalski, *Anal. Chem.* **59**, 1529 (1987).
4. T. A. Dickinson, D. R. Walt, J. White, J. S. Kauer, *Anal. Chem.* **69**, 3413 (1997).
5. . E. T. Zellers, J. Park, T. Hsu, W. A. Groves, *Anal. Chem.* **70**, 4191 (1998).
6. S. W. Wenzel and R. M. White, *Sensors and Actuators* **A21-23**, 700 (1990).
7. R. M. White, P. J. Wicher, S. W. Wenzel, and E. T. Zellers, *IEEE Trans. Ultrasonics,Ferroelectrics, and Freq. Control*, **34**, 163 (1987).
8. E. T. Zellers, R. M. White, and S. W. Wenzel, *Sensors and Actuators*, **14**, 35 (1988).
9. J. Grate, S. W. Wenzel, R. M. White, *Anal. Chem.*, **63**, 1552 (1991).
10. D. S. Ballantine, R. M. White, S. J. Martin, A. J. Ricco, G. C. Frye, E. T. Zellers, H. Wohltjen, *Acoustic Wave Sensors: Theory, Design, and Physicochemical Applications,* Academic Press, Boston, MA (1996).
11. W. A. Groves, E. T. Zellers, G. C. Frye, *Anal. Chim. Acta* **371**, 131 (1998).
12. J. Park, G.-Z. Zhang, E. T. Zellers *Am. Ind. Hyg. Assoc. J.* 1999 (in press).
13. J. W. Grate, S. L. Rose-Pehrsson, D. L. Venezky, M. Klusty, H. Wohltjen. *Anal. Chem.*, **65**, 1868 (1993).
14. J. Grate, M. Abraham, *Sens. Actuators B*, **3**, 85 (1991).
15. J. Park, W. A. Groves, E. T. Zellers, *Anal. Chem.* 1999 (in press).
16. E. T. Zellers, manuscript in preparation.
17. J. W. Grate, S. J. Patrash, S. Kaganove, B. N. Wise, *Anal. Chem*, **71**, 1033 (1999).

# THE SENSITIVITY OF $WO_3$ THIN FILMS TO $O_3$, $NO_2$ AND $Cl_2$ GASES

C. Cantalini
Dept.of Chemistry and Materials, 67040, Monteluco di Roio, L'Aquila, Italy
S. Santucci, M. Passacantando
Dept. of Physics and INFM L'Aquila, 67010 Coppito, L'Aquila, Italy
E. Comini, G. Faglia and G. Sberveglieri
Dept. di Chimica Fisica per l'Ingegneria and INFM, Via Valotti, 9, 25133 Brescia , Italy
Y. Li, W. Wlodarski
Dept. of Communication and Electronic Engineering, RMIT University
Victoria.3001, Melbourne, Australia

$WO_3$ thin films have been prepared by Sol-Gel (SG), Radio Frequency Sputtering (RFS) and Vacuum Thermal Evaporation (VTE) techniques on alumina substrates and annealed at 600°C for 24 h in air. The morphology, crystalline phase and chemical composition have been characterized using SEM, XRD and XPS techniques. The electrical response has been measured by exposing the films to $O_3$ (10 to 180 ppb), $NO_2$ (0.2 to 1 ppm) and $Cl_2$ (0.1 to 1 ppm) and operating temperatures between 150°C and 450°C and 50% humid air. The response to $O_3$ has been found to be at maximum at 400 °C. At this temperature that of $NO_2$ and $Cl_2$ is negligible. Improvements on the $O_3$ gas sensitivity and selectivity can be achieved by fixing the operating temperature at 400 °C. The most recommended temperature for $NO_2$ and $Cl_2$ detection has resulted to be 200 °C.

## INTRODUCTION

Transition-metal oxides represent a very interesting class of materials because of their potential applications as catalysts and sensors (1) Among them tungsten oxide ($WO_3$) thin films have been extensively studied as prototypes of electrochromic devices and gas sensors due to their excellent electrical and optical properties.(2-3).

Previous research has established that the $WO_3$ sensors prepared by sol-gel (4), vacuum thermal evaporation (5) and radio frequency sputtering (6), are characterized by high sensitivity to sub-ppm levels of $NO_2$. Oxidizing gases such as $NO_2$, $Cl_2$, and $O_3$ cause the sensor resistivity to increase. This is generally the case for n-type semiconductor oxide sensors.

In order to asses $WO_3$ sensor for $O_3$ monitoring ($O_3$ safety level is about 50 ppb), very high sensitivities and selectivities are required to avoid cross interfering with other oxidizing gases like $NO_2$ and $Cl_2$. The preparation of $WO_3$ thin film sensors with the ability to detect $O_3$ with high selectivity in the presence of nitrogen compounds, hydrocarbons and possibly VOC (photochemical smog), represent the actual challenge for the application of $WO_3$ semiconductor oxides for urban air quality monitoring.

This paper reports on the electrical response to $O_3$ (10 - 180 ppb), $NO_2$ (0.2 – 1 ppm) and $Cl_2$ (0.2 –1ppm) of $WO_3$ thin films prepared by SG, RFS and VTE techniques.

## EXPERIMENTAL

RFS were deposited on alumina substrates starting from a tungsten and titanium (90%:10%, in weight) target in a reactive atmosphere of oxygen and argon ($P_{O2}=2\times10^{-3}$ mbar, $P_{Ar}=2\times10^{-3}$ mbar) with the substrate held at 300°C. After the deposition, the films underwent an annealing cycle in air at 600°C for 30 hrs.

SG were prepared by mixing tungsten ethoxide ($W(OC_2H_5)_6$, 99.9% purity) in *n*-butanol (0.2 M solution). After ultrasonic agitation, the prepared solution was spun at 2500 rpm for 30 sec onto an alumina substrate. The thin films, after aging overnight at room temperature were annealed for 1 hr in static air at 600°C.

VTE were prepared by heating a commercial $WO_3$ powder with 99.995% purity under vacuum at $5\times10^{-4}$ Pa. The vapor phase was condensed on the alumina substrate. Annealing was performed in air at 600°C for 24 hrs.

The electrical sensing properties of the $WO_3$ thin films to $O_3$ gas were measured by an automated system. Air from certified bottle was humidified at 50 % r.h and fed into an ozone generator (up to 500 ppb) based on a thermostated UV lamp discharge. $NO_2$ and $Cl_2$ mixtures have been obtained by diluting the gases with humid air and controlling the gas composition by MultiRAE gas monitor system (RAE Systems CA). The gas response $S$ is defined as $S=R_g/R_a$, where $R_g$ and $R_a$ are the electrical resistances in gas and in air.

## RESULTS AND DISCUSSION

### Microstructure

XRD diffraction investigation highlights the formation of well crystallized microstructures after annealing at 600 °C for all the prepared films. The VTE and SG are oriented with preferential growth along the [200] crystallographic plane of monoclinic $WO_3$ (JCPDS no. 43-1035). The RFS thin film shows a crystallographic peak orientation close to the tetragonal phase of $WO_3$ (JCPDS no. 20-1324). No diffraction peaks belonging to any crystalline phase of $TiO_2$ has been detected for the RFS film.

XPS characterization of the SG film shows, the occurrence of negligible contamination of the surface due to incomplete organic carbon removal at high temperature. RFS and VTE films seem to be not contaminated since no peaks, than the characteristics W and O, with the only exception of Ti 2p peak for the RFS film, have been detected.

SEM investigations of the SG film reveal a uniform, continuous and with an "orange skin" appearance micro-cracks free surface. SEM of the VTE film shows, on the other hand, the occurrence of extended surface cracks. These cracks are believed not to propagate through the whole thickness of the film, since no $Al_{2p}$ reflection coming from the substrate have been detected by detailed XPS measurements. SEM of the RFS film shows a well compact structure of equiaxed grains, and relatively large $WO_3$ crystallites segregating along the grain boundaries.

### Electrical Properties

Gas sensing characterisation has been carried out at 200°C and 400 °C in wet air (50 % R.H. at 20 °C) and exposing the films to three different atmospheres, namely: $O_3$ (10-200 ppb), $NO_2$ (0.2-1 ppm) and $Cl_2$ (0.4 –1 ppm).

Figure 1 shows the electrical response of the films in 50% R.H air carrier at 400 °C operating temperature when the $O_3$ concentration is changed from 10 to 130 ppb. The response to different ozone concentrations at 200 and 400 °C operating temperatures,

expressed as $S = R_G/R_A$, is reported in Fig.2. From this figure it turns out that SG film yields a higher response at 400 °C than at 200 °C operating temperature.

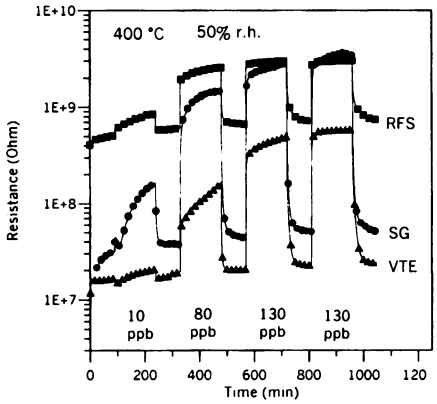


Fig.1 $O_3$ response at 400 °C

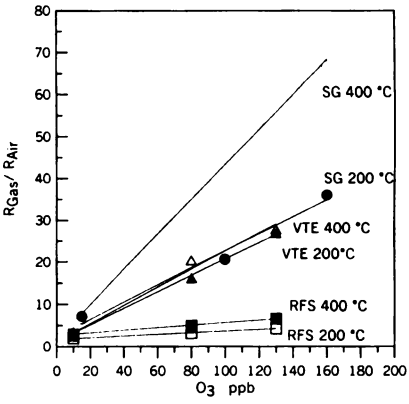


Fig.2 $O_3$ Sensitivity at 200 and 400 °C

VTE and RFS films, considering the experimental error and signal reproducibility, do not show significant variation of S with the working temperature. For a given operating temperature, here it is clearly evident how the chemical preparation route enhances the $O_3$ response as respect to the films prepared by physical methods.

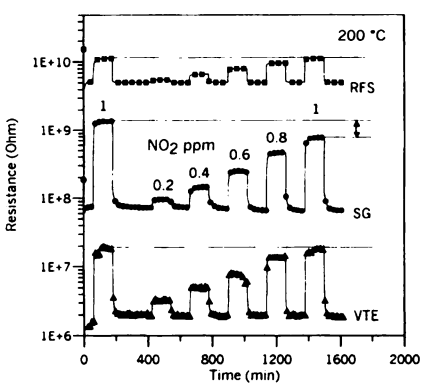


. Fig.3 $NO_2$ response at 200 °C

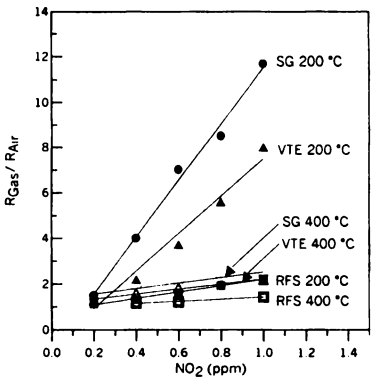


Fig.4 $O_3$ Sensitivity at 200 and 400 °C

Figure 3 shows the response of the films at 200 °C and different $NO_2$ concentrations. The test has been carried by exposing the film to the maximum gas concentration (1 ppm $NO_2$), followed by a dynamic adsorption-desorption cycle, by increasing stepwise the $NO_2$ gas concentration. SG film yields higher resistance when exposed to 1 ppm $NO_2$ for the first time, as compared to the resistance obtained at 1 ppm $NO_2$ at the end of the dynamic conditioning. Arrows in the figure highlight the difference of the measured resistance at saturation and 1 ppm $NO_2$. Physical prepared films are highly reproducible throughout the experimental sequence and $NO_2$ concentrations.

The response to different $NO_2$ concentrations and operating temperatures, is reported in Fig.4. The $NO_2$ response is for all the films at maximum at 200 °C.

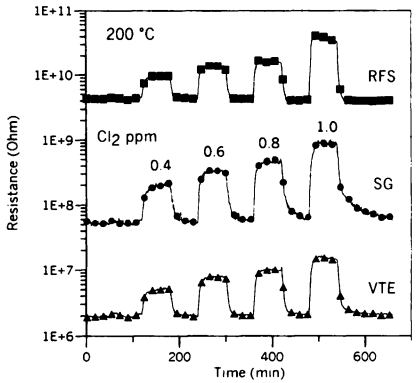


Fig.5 $Cl_2$ response at 200 °C

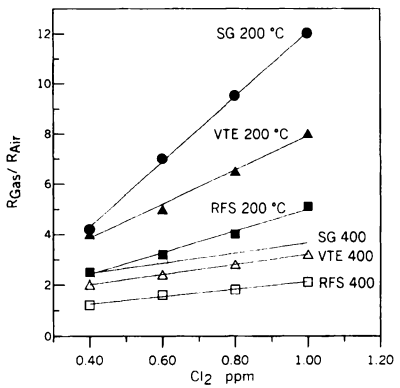


Fig.6 $Cl_2$ Sensitivity at 200 and 400 °C

Figure 5 shows the electrical response of the films in 50% R.H air carrier and 200 °C operating temperature when the $Cl_2$ concentration is changed stepwise from 0.4 to 1 ppm. RFS prepared has resulted to be the faster to respond and the more stable in terms of signal reproducibility. The response to different $Cl_2$ concentrations and operating temperatures, is reported in Fig.6. The $Cl_2$ response is at maximum at 200 °C.

## CONCLUSIONS

$WO_3$ material prepared by sol-gel, vacuum thermal evaporation and r.f. sputtering shows potential application for the measure of $O_3$ in the 10 –160 ppb concentration range.

SG prepared films have shown greater sensitivities as respect to VTE and RFS for all the investigated gases and operating temperatures.

The response to $O_3$ has been found to be at maximum at 400 °C for the SG while not much affected by temperature for the VTE and RFS films. The $NO_2$ and $Cl_2$ response is for all the films at maximum at 200 °C. Improvements on the $O_3$ gas sensitivity and selectivity can be achieved by fixing the operating temperature of the films at 400 °C.

## REFERENCES


1. H.H. Kung, *Transition Metal Oxides: Surface Chemistry and Catalysis*, **45**, p. 259, Elsevier (1989).
2. K. Von Rottkay, M. Rubin, and S.J. Wen, *Thin Solid Films*, **306,** 10 (1996).
3. M. Akiyama, Z. Zhang, J. Tamaki, T. Harada, N. Miura and N. Yamazoe, *Tech. Digest 11th Sensor Symp.*, Japan, p.181, (1992).
4. X. Wang, G. Sakai, K. Shimanoe, N. Miura, N. Yamazoe, *Sensors and Actuators,* **B45**, 141 (1997).
5. C. Cantalini, H.T. Sun, S. Santucci, M.Passacantando, *Sensors and Actuators,* **B35-36**, 112 (1996).
6. M. Ferroni, V. Guidi, G. Martinelli, P. Nelli, G. Sberveglieri, *Sensors and actuators,* **B 44**, 499 (1997)

# CHEMICAL SENSORS IV


Edited by
M. Butler
N. Yamazoe
P. Vanysek
M. Aizawa

# CHEMICAL SENSORS IV

*Proceedings of the Symposium*

## Editors

M. Butler
Sandia National Laboratories
Albuquerque, New Mexico

N. Yamazoe
Kyushu University
Fukuoka, Japan

P. Vanysek
Northern Illinois University
DeKalb, Illinois

M. Aizawa
Tokyo Institute of Technology
Yokohama, Japan

*THE SENSOR DIVISION*

**Proceedings Volume 99-23**

THE ELECTROCHEMICAL SOCIETY, INC.,
10 South Main St., Pennington, NJ 08534-2896, USA

Published by:

The Electrochemical Society, Inc.
10 South Main Street
Pennington, New Jersey 08534-2896, USA

Telephone 609.737.1902
Fax 609.737.2743
e-mail: ecs@electrochem.org
Web: http://www.electrochem.org

Library of Congress Catalogue Number: 99-65336

ISBN 1-56677-246-X

Printed in the United States of America